ACS FOOD SCIENCE & TECHNOLOGY

pubs.acs.org/acsfoodscitech

Article

One-Pot Fabrication of Chitosan/Poly(vinyl alcohol) Films with *Spondias Pinnata* Fruit Extract-Mediated Silver Nanoparticles for Meat Preservation

Tilak Gasti,* Shruti Dixit, Lokesh A. Shastri, Bhagyavana S. Mudigoudra, Ravindra B. Chougale,* and Saraswati P. Masti

Cite This: *ACS Food Sci. Technol.* 2025, 5, 2430−2443

Read Online

ACCESS | Metrics & More | Article Recommendations | Supporting Information

ABSTRACT: The need for green, simplified, and single-step synthesis process, rather than a multistep approach for nanocomposite films, has received much interest recently. Hence, the current work aims to develop a one-pot green fabrication method for chitosan (CS)/poly(vinyl alcohol) (PVA)/Ag nanocomposite (CPAg) films, using *Spondias pinnata* fruit pulp extract (SPFPE) as a silver ion reducing agent, with the CS/PVA matrix being used as both a capping and stabilizing agent. The generation of AgNPs within the CS/PVA matrix was confirmed by the dark brown color of the films and the UV−visible absorption peak at 443 nm. This was further corroborated by X−ray diffraction and SEM−EDS analyses. The CPAg nanocomposites had improved mechanical strength by 19.55% compared to the pure CS/PVA. The incorporation of AgNPs along with the SPFPE enhances the anti-UV radiation efficiency, surface hydrophobicity, and water vapor transmission rate, and the films undergo rapid biodegradation (>36%) in untreated soil. In addition, the overall migration limit of the CPAg nanocomposite film was found to be below the permitted limit of 10 mg·dm^{-2} against three food simulants. Nevertheless, CPAg nanocomposite films exhibited strong antioxidant activity against DPPH free radicals and had the potential to inhibit the growth of foodborne pathogens like *B. cereus*, *E. coli*, *P. aeruginosa*, *S. aureus*, and *C. albicans*. Further, the CPAg-2 film remarkably extended the shelf life of lamb meat up to 30 days when stored at 4 °C. Thus, the prepared nanocomposite films have fulfilled the prerequisite properties for potential packaging materials in the meat industry.

KEYWORDS: *chitosan, poly(vinyl alcohol), AgNPs, meat packaging, shelf life, fruit extract*

1. INTRODUCTION

Consumer demand for safe and fresh food products continues to rise. According to the United Nations Food and Agriculture Organization (UNFAO), about one-third of all food produced globally is wasted every year. This food wastage is directly connected to excessive buying and poor packaging systems.[1] As a result, United Nations member states have pledged to meet the Sustainable Development Goal (SDG) of decreasing food loss and waste by 50% by 2030.[2] Achieving this target requires coordinated global efforts to improve food storage and packaging systems. It is becoming increasingly challenging to supply plant-based, healthy cuisine to people around the world due to rising population demand. Consequently, most countries rely on meat as a primary source of protein and calories. However, meat storage and preservation are challenging due to rapid microbial growth, which causes the meat to spoil. The preservation of packaged meat products has become a serious concern, even when kept under advanced conditions, such as cold storage and a vacuum atmosphere. Therefore, it is essential to develop sustainable materials that not only protect the quality of meat but also increase its shelf life.

In the past decade, the appearance of a large number of reports on naturally derived polymer films for active food packaging applications has highlighted the need for sustainable materials for food preservation and shelf-life extension. The biodegradable nature of these macromolecules is a key factor in choosing them for packaging purposes. In order to minimize the environmental hazards caused by petroleum-derived packaging materials, they have been replaced by biobased macromolecules. In this context, natural polymer-based active films, apart from being degradable and nontoxic, are proficient at migrating antioxidants without causing any unwanted contamination. The majority of the biopolymer films are produced from agro-waste and byproducts from seafood products. Due to the strong film-forming ability, barrier to UV−visible light and oxygen, and high tensile properties of several abundant biopolymers such as cellulose, starch, alginates, and chitosan, they have been widely used in food packaging applications.[3] Among them, chitosan has been extensively implemented in the field of active packaging due to its abundance, eco-friendly nature, low cost, and ease of handling.

Chitosan (CS) is the second most abundant biopolymer on the planet, next to cellulose, and is made from the

Received: March 10, 2025
Revised: May 6, 2025
Accepted: May 8, 2025
Published: May 15, 2025

deacetylation of chitin extracted from shellfish.[4] The presence of positively charged, active amino groups on the polysaccharide chain makes CS a natural antimicrobial agent. Based on its antibacterial and antifungal properties, chitosan is widely used in active packaging systems. The implementation of CS coatings or films has significantly extended the shelf life of packaged green vegetables and fruits, meat products, dairy products, and marine food products.[5] Despite these advantages, CS has some drawbacks due to its brittleness, acidic instability, and limited flexibility.[6] To overcome these limitations, chitosan is often blended with degradable synthetic polymers.

Poly(vinyl alcohol) (PVA) is a synthetic, semicrystalline, water-soluble polymer that has a strong film-forming capacity. It has many beneficial properties, including high transparency, chemical stability, high mechanical strength, biocompatibility, and degradability.[7] The availability of excess hydroxyl groups on the polymer chain facilitates intramolecular hydrogen bonding, which enhances its mechanical properties. Among synthetic polymers, PVA is highly favored due to its broad use in various fields, including biomedical applications, textiles, membranes, and food packaging.[8] However, the properties of undoped and neatly blended films have not been sufficient for food packaging. In order to enhance the multifunctional properties of blended films, nanoadditives or nanofillers have been incorporated into the polymer matrices.

Nanoparticles are key functional materials used in various research sectors. Nanoparticles have received great attention due to their wide range of applications, such as drug delivery, catalysis, and antimicrobial packaging systems.[9] In recent years, several nanoparticles, such as zinc oxide, copper oxide, titanium, silica, and silver nanoparticles, have been successfully utilized in food packaging materials.[10,11] Among these, silver nanoparticles (AgNPs) are considered the most prominent due to their large surface area, low toxic effect on humans, and ability to damage the cell walls of harmful microbes.[12] The *ex situ* and *in situ* approaches to incorporating AgNPs into packaging materials are both viable options. The *in situ* generation of AgNPs offers several advantages, including excellent stability, homogeneous dispersion, and reduced particle agglomeration. Several methods have been reported for synthesizing AgNPs, including the chemical reduction method and the green reduction method. However, the chemical reduction method is carried out using hydrazine hydrates and sodium borohydride, but these reducing agents left a harsh residue on the AgNPs surface, causing toxicity. Hence, the green reduction method, using plant extracts such as olive fruit[13] and *Cotoneaster nummularia*,[14] was used to avoid the deposition of harsh chemicals on the AgNPs' surface. The use of natural extracts in the development of eco-friendly nanopackaging films not only aids in nanoparticle synthesis but also acts as a green preservative due to the presence of polyphenols and flavonoids. For example, anthocyanin extracted from fruits and vegetables has significantly extended the shelf life of the packaged food products.[15,16] Furthermore, PVA/gelatin film infused with Amaranthus leaf extract has significantly improved the shelf life of fish and chicken due to the high antioxidant capacity of the phytochemicals in the Amaranthus leaf.[17] In this context, the use of natural extracts in the development of food packaging systems is considered to be a highly effective choice.

Spondias pinnata (S. pinnata), also known as Indian hog plum or wild mango, belongs to the Anacardiaceae family and is commonly found in India, Sri Lanka, Thailand, and Malaysia.[18] In India, unripe fruits of *S. pinnata* are frequently used to make pickles, while young leaves, flowers, and fruits are all edible. Its root bark and fruits hold significant value in traditional medicine.[19] This member of the Anacardiaceae family exhibits beneficial pharmacological properties, such as anti-inflammatory, anticancer, and photoprotective effects.[20] The major phytochemicals present in the *S. pinnata* fruit include gallic acid, ascorbic acid, beta-amyrin, oleanolic acid, amino acids such as glycine, cystine, serine, alanine, and leucine, and acidic polysaccharides.[21] These phytochemicals have the ability to inhibit the growth of foodborne pathogens and reduce oxidative spoilage,[22] making *S. pinnata* extract-based materials a promising alternative to synthetic preservatives and conventional plastic packaging. In addition to its functional benefits, the use of *S. pinnata* aligns with the global push for eco-friendly and biodegradable materials in response to increasing concerns over plastic waste. Based on these beneficial properties, *S. pinnata* fruit extract is a promising additive for the sustainable development of food packaging systems.

It has been reported that the incorporation of AgNPs enhances the physicomechanical properties and also provides effective antimicrobial properties to the CS/PVA films.[23] There are several studies that have explored AgNPs integrated into CS/PVA blended matrices. For instance, Ragab et al. (2024) developed poly(vinyl alcohol) (PVA)/chitosan (CS) film incorporated with green-synthesized silver nanoparticles (AgNPs), demonstrating improved thermal and antibacterial properties.[24] Similarly, the integration of aloe vera-mediated AgNPs into the CS/PVA matrices showed enhanced mechanical strength and antimicrobial efficiency.[25] However, this method is multistep and time-consuming. Additionally, the external addition of presynthesized nanoparticles into the polymer matrices often presents several drawbacks, such as poor dispersion, particle agglomeration, and weak bonding interactions.[26] These limitations can adversely affect the mechanical strength, transparency, and overall functional properties of the resulting films.[27] On the other hand, one-pot synthesis enables an *in situ* synthesis mechanism that facilitates higher dispersion and stronger interaction between the nanoparticles and polymer matrices. This method not only enhances the molecular interactions but also improves the functional properties of the resulting films.

This research aims to bridge that gap by conducting a proximate analysis of *S. pinnata* fruit pulp extract and utilizing it for the one-pot green synthesis of AgNPs within a CS/PVA matrix. In this process, the synthesis of AgNPs and their incorporation within the CS/PVA polymer blend matrix occur simultaneously in a single reaction vessel. This method significantly eliminates the need for separate synthesis and purification steps, thereby reducing the time and simplifying the process. Herein, *S pinnata* fruit pulp extract is used as a reducing agent, and CS and PVA are used as stabilizing and capping agents. The further objective of this work is to investigate the combined effect of AgNPs and phytochemicals present in *S. pinnata* fruit pulp extract on the physicochemical and biological properties of the CS/PVA films for active food packaging applications, especially for lamb meat packaging and preservation.

https://doi.org/10.1021/acsfoodscitech.5c00238
ACS Food Sci. Technol. 2025, 5, 2430−2443

2. MATERIALS AND METHODS

2.1. Materials. The ripened fruits of *Spondias pinnata* were collected from the local area of Dharwad, Karnataka, India. Low molecular weight chitosan (degree of deacetylation 75−85%, viscosity 5−20 mPa s) was procured from Tokyo Chemical Industry, Japan. Poly(vinyl alcohol) with a molecular weight of 15 kDa (degree of hydrolysis 98−99%) and the required microbial media were obtained from Loba Chemie, India. Sodium carbonate and acetic acid (AR) were purchased from SD Fine Chemicals, India. $AgNO_3$ (AR) was purchased from Thomas Baker Pvt. Ltd., India. Folin-Ciocalteu reagent, gallic acid, rutin, and 1,1-diphenyl-2-picrylhydrazyl (DPPH) were procured from Sigma-Aldrich, India. All chemicals and reagents were used as received, and Millipore water was used throughout the work.

2.2. Methods. *2.2.1. Preparation S. pinnata Fruit Pulp Extract (SPFPE).* The conventional refluxing method was used to prepare the extract. Ripened *S. pinnata* fruits were gently washed with Millipore water, and the skin was removed. About 25 g of pulp was placed in a 250 mL round-bottom flask containing 100 mL of Millipore water. The refluxing was carried out at 60 ± 2 °C for 4 h. A light yellow extract was filtered three times using Whatman filter paper No. 1 to avoid pulp residue, then concentrated in a water bath, and stored at 2 ± 1 °C until further use.

2.2.2. Preparation of CS/PVA/Ag Nanocomposite Films. The solvent casting method was used to prepare the CS/PVA/Ag nanocomposite films. Typically, a known weight of CS was dissolved in a 80 mL of 2% acetic acid solution (w/v) and filtered to remove undissolved particles. PVA was dissolved in 40 mL of hot Millipore water by using a magnetic stirrer. Both CS and PVA solutions were mixed and stirred for 2 min. Thereafter, different weight percent of $AgNO_3$ and *S. pinnata* fruit pulp extract were added while stirring, as mentioned in Table S1. After stirring for 37 min, the color of the reaction mixture changed from light yellow to dark brown (Figure 1),

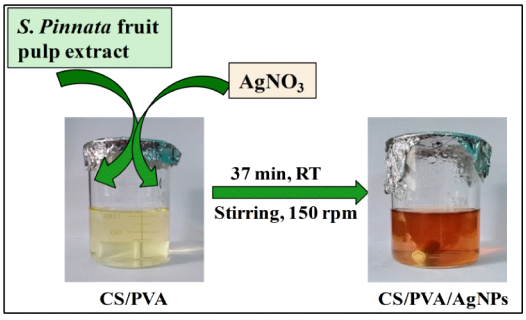

Figure 1. Formation of AgNPs in CS/PVA solution.

which indicates the formation of AgNPs.[28] The silver ions (Ag^+) were reduced to metallic silver (Ag^0) by bioactive compounds present in the fruit pulp, such as flavonoids, ascorbic acid, phenolics, and tannins, which act as natural reducing agents. These phytochemicals donate electrons to reduce Ag^+ ions, initiating nanoparticle formation (Figure 2). Concurrently, amino groups of CS and hydroxyl groups of PVA bind to the AgNPs' surface, preventing particle agglomeration and promoting uniform distribution, thereby acting as capping and stabilizing agents. The resulting homogeneous solution was degassed using an ultrasonication bath, followed by casting on glass Petri plates, and allowed to dry at room temperature for 4 days. The dried films were peeled off and stored in a desiccator containing anhydrous calcium chloride. To assess the influence of CS/PVA on AgNPs formation, the reaction was carried out without *S. pinnata* fruit pulp extract for 24 h at room temperature, and no color change was observed. This indicates that *S. pinnata* fruit pulp extract readily reduces the Ag^+ ions to Ag^0, and CS/PVA matrices behave as stabilizing as well as capping agents.

2.2.3. Determination of Total Phenolic and Total Flavonoid Contents. The total phenolic content of the *S. pinnata* fruit pulp extract was determined as the gallic acid equivalents per 100 g (mg GAE/g) of dry powder spectrophotometrically, according to the Folin−Ciocalteu (F−C) method.[29] An aliquot of the extract (125 μL) was added to the F−C reagent (1.8 mL) and mixed thoroughly, after which it was incubated at room temperature for 5 min. After this, a 15% (w/v) sodium carbonate solution (1.2 mL) was added. The samples were vortexed and allowed to stand at room temperature for 1.5 h. The absorbance of the colored solution was measured at 765 nm by using a UV−vis spectrophotometer (PerkinElmer LAMBDA 360). The total phenolic content was determined from the standard (50−500 mg/mL) calibration curve ($Y = 0.0024x - 0.1382$, $R^2 = 0.9475$) of gallic acid. The total phenolic content of the *S. pinnata* fruit pulp water extract was found to be 130.92 ± 0.7 mg of GAE/100 g.

2.2.4. Proximate Nutrient Analysis of S. pinnata Fruit. The proximate analysis was employed to estimate the amount of moisture, crude fiber, ash, total fats, and carbohydrate content of the SPPE. The crude protein content was measured by the Kjeldahl nitrogen method,[30] while ash, total fats, and moisture content were appraised in accordance with the Association of Official Analytical Chemists (AOAC). The difference between the dry weight and ash content of the residue was used as an approximation of the crude fiber content. The total carbohydrates were estimated by the difference method as 100% − (% moisture) − (% protein) − (% fat) − (% ash).[31]

2.3. Film Properties. Confirmation of synthesized AgNPs and optical properties, such as opacity and transparency, of the prepared nanocomposite films were carried out using UV−Vis spectrophotometry (PerkinElmer LAMBDA 360). Film sample with uniform thickness (2 × 2 cm^2) was inserted into a sample chamber using air as

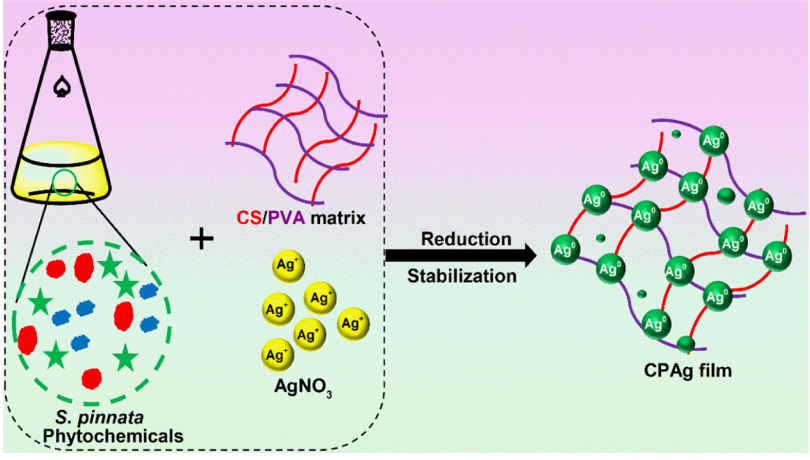

Figure 2. Mechanism of AgNPs formation and interaction between the film components.

https://doi.org/10.1021/acsfoodscitech.5c00238
ACS Food Sci. Technol. 2025, 5, 2430−2443

the standard reference at room temperature. The spectrum was recorded between the wavelengths of 200 and 800 nm. Opacity and transparency were calculated according to our previous report.[32] Three measurements were taken for each sample, and the results were expressed as mean standard deviation.

A scanning electron microscope equipped with energy-dispersive X-ray spectroscopy (SEM-EDS) (Zeiss sigma 360) was used to analyze the surface topography and elemental analysis. Before analysis, the film sample was placed on a specimen holder and sputter-coated with a gold layer. The screening was carried out at a 5 kV accelerating voltage.

The crystalline/amorphous nature of the prepared nanocomposite films was investigated using an X-ray diffractometer (XRD) (Rigaku SmartLab, Japan). Each film sample (2.5 × 2.5 cm^2) was placed on a specimen holder for the analysis. An X−ray beam originating from a copper target Cu Kα (λ =1.5418 Å) source at a voltage of 30 kV and a current of 20 mA was used to scan the sample over the angular range from 2θ = 5−80° with a scanning rate of 5° min^{-1}. The degree of crystallinity (X_C %) of the nanocomposite films was calculated using eq 1.

$$X_C\% = \frac{\text{Area of crystalline peaks}}{\text{Total area of all peaks}} \times 100 \quad (1)$$

The FT−IR spectra of prepared active nanocomposite films were recorded by using an attenuated total reflection (ATR) infrared spectrometer (Thermo Fisher, Nicolet iZ10, USA). The spectra were recorded in the range of 400−4000 cm^{-1} at ambient temperature with a spectral resolution of 4 cm^{-1}.

The surface wettability of the prepared nanocomposite films was analyzed by a sessile drop method using a contact angle meter (Model DMs−401, Kyowa Interface Science, Tokyo). A drop of distilled water was deposited on the film surface (2 × 2 cm^2) using a micro syringe, and the static contact angle of the water droplet was measured using preinstalled software. Four measurements for each film sample were performed, and the average along with the standard deviation was reported.

Moisture absorption (MA) at equilibrium and moisture retention capacity (MRC) of the prepared nanocomposite films were determined according to the ASTM D570−98 (2018) standard. Briefly, the film samples (2 × 2 cm^2) are dried in an oven at 40 °C for 12 h and then placed in a desiccator to cool. Immediately upon cooling, the samples are weighed. The sample is then exposed to atmospheric conditions at 23 °C until equilibrium was achieved and weighed again. MA (%) and MRC (%) were calculated by using eqs 2 and 3, respectively.

$$MA\% = \frac{W_2 - W_1}{W_1} \times 100 \quad (2)$$

$$MRC\% = \frac{W_2}{W_1} \times 100 \quad (3)$$

Where, W_1 and W_2 are the initial dry weight (g) and final wet weight (g) after exposure to atmospheric conditions, respectively.

To determine the water solubility (W_S) of the films, the method of Zimet et al. (2019) was employed with some modifications.[33] The film samples (2 × 2 cm^2) were dried at 50 ± 2 °C for 72 h and weighed. The weighed film samples were placed in 40 mL of Millipore water and were allowed to stir at room temperature for 24 h. The undissolved film samples were then filtered and dried at 80 ± 2 °C until reaching a constant weight to determine the final dry weight. Film solubility (%) was calculated using eq 4.

$$W_S(\%) = 100 \times \frac{W_i - W_f}{W_i} \quad (4)$$

Where, W_i and W_f are the initial dry mass and final dry mass of the films, respectively.

The soil burial test was carried out according to our previous report[34] and the percent soil degradability ($\%S_D$) was calculated using eq 5.

$$\%S_D = \frac{\text{Film weight}_{\text{initial}} - \text{Film weight}_{\text{final}}}{\text{Film weight}_{\text{initial}}} \times 100 \quad (5)$$

2.4. Mechanical Properties. The tensile properties of the prepared films were investigated by using a universal testing machine (DAK Systems ASTM D882−91). The film sample (2.5 × 10 cm^2) was placed in a grip holder with a separation of 5 cm and stretched at a crosshead speed of 1 mm/min. The stress-versus-strain curves were used to determine the tensile strength, elongation at break, and tensile modulus.

2.5. Water Vapor Transmission Rate (WVTR). The water vapor transmission rate of the prepared nanocomposite films was evaluated according to the previous report.[35] Briefly, 3 × 3 cm^2 film samples were placed on the circular mouth (1.7 cm diameter) of a glass bottle containing 10 mL of Millipore water and tightened with Teflon tape. The initial weight of the bottle was measured (W_i) and placed in an hot air oven at 40 °C. After 24 h, the sample bottles were withdrawn from the oven and weighed again (W_f). The WVTR was calculated using eq 6.

$$WVTR = \frac{W_i - W_f}{\text{Area of mouth of the bottle}} \times \text{Time} \quad (6)$$

2.6. Overall Migration Limit (OML) Test. The overall migration limit (OML) of the prepared films was determined according to the IS: 9485 (1998) standards. Distilled water, 3% acetic acid, and 50% ethanol were used as food simulants to imitate the behavior of aqueous, acidic, and alcoholic beverage products, respectively. Preweighed film (2 × 2 cm^2) samples were immersed in each beaker containing 30 mL of simulants and kept in a hot air oven at 40 °C for 10 days. After 10 days, the film samples were withdrawn from the beakers, and the stimulants were evaporated to dryness. The weight of the residue was recorded, and the OML was calculated gravimetrically. The results were expressed in mg dm^{-2}.[22]

2.7. Antioxidant Activity. The free radical scavenging activity of the prepared films was carried out using the 1,1−diphenyl−2−picrylhydrazyl (DPPH) assay. In a test tube, 2 mL of DPPH solution (0.01 M in methanol) and 1 mL of film sample with different concentrations (20−100 mg/mL) were gently mixed, allowed to stand in a dark place for 30 min, and incubated at 36 °C. Thereafter, the reaction mixture was exposed to UV−visible spectroscopy at an absorbance of 517 nm. The above-mentioned protocol was also employed to ascorbic acid used as a standard reference, and blank DPPH (without sample) was used as a control. DPPH radical scavenging assay was calculated using eq 7.

$$\text{Scavenging assay}(\%) = \frac{\text{DPPH}_{\text{Absorbance}} - \text{Sample}_{\text{Absorbance}}}{\text{DPPH}_{\text{Absorbance}}} \times 100 \quad (7)$$

2.8. Antimicrobial Activity. The microbial resistance ability of prepared nanocomposite films against common foodborne pathogens, such as Gram-positive *Staphylococcus aureus*, *Bacillus cereus*, and Gram-negative *Escherichia coli*, *Pseudomonas aeruginosa*, and fungi *Candida albicans* was assessed using the agar disc diffusion method.[36] The freshly prepared bacterial cultures were incubated at 37 ± 1 °C for 24 h. Then, 100 μL of incubated bacteria and fungi cultures (10^5 CFU/mL) suspension was inoculated onto the nutrient agar and potato dextrose agar plates, respectively. Then, the prepared films (1 × 1 cm^2) were placed on labeled, sterile plates. The inoculated plates were incubated for 12 h at 37 ± 1 °C and 29 ± 1 °C for antibacterial and antifungal activities, respectively, followed by observation of the zones of inhibition around or below the film samples.

2.9. Lamb Meat Packaging Test. *2.9.1. Estimation of Total Psychrotrophic Bacterial Count.* The boneless lamb meat was brought from a local slaughterhouse and then immediately transferred to the laboratory under aseptic conditions to prevent contamination. The obtained meat sample was stored at 4 °C until a test was performed. The film samples CS/PVA, CPPFE, and CPAg-2 were selected for the packaging study. Around 20 g of the meat sample was wrapped with 5 × 10 cm^2 film samples and packed individually in a

https://doi.org/10.1021/acsfoodscitech.5c00238
ACS Food Sci. Technol. 2025, 5, 2430−2443

polyethylene ziplock pouch. The packed lamb meat samples were stored at 4 °C for 30 days. The bacterial count was estimated on days 0, 3, 6, 9, 12, 15, and 30. For psychrotrophic bacterial growth in lamb meat, the packed meat samples were aseptically homogenized for 60 s in a stomacher with 90 mL of 0.1% peptone water. In duplicate, 1 mL aliquots of serially diluted homogenate were plated. Plates were incubated for 48 h at 37 °C, followed by colony counting. The results were expressed in log cfu/g.[37]

2.9.2. Estimation of Lipid Peroxidation. Lipid peroxidation of meat wrapped with CS/PVA, CPPFE, CPAg-2 films, and unwrapped meat samples was determined on days 7, 15, and 30 according to the AOCS 965.33 official method.[38] Briefly, the unwrapped meat sample was minced and extracted using a Soxhlet extraction with *n*-hexane. Then, the extracted fat (1 mg), 6 mL of a chloroform-acetic acid mixture (2:3 *v*/v), a saturated solution of potassium iodide (1 mL), and distilled water (6 mL) were added to a 100 mL Erlenmeyer flask. The whole reaction mixture was thoroughly mixed. After competitive mixing, 1% starch (1 mL) solution was added. Then, the mixture was titrated against 0.01N sodium thiosulfate until the color changed from bluish-black to colorless. The total peroxide value (PV) was calculated by using eq 8. Peroxide values are expressed in mequiv/1000 g of lipid.

$$\mathrm{PV} = \frac{V \times N \times 1000}{W} \tag{8}$$

where V is the volume of the sodium thiosulfate consumed during titration, N is the normality of the sodium thiosulfate, and W is the weight of the fat used.

2.10. Statistical Analysis. Film properties were measured in triplicate, and results were expressed as mean ± SD. One-way analysis of variance (ANOVA) and Tukey's test ($p \leq 0.05$) were employed to detect significant differences among the mean values, using Origin 9 software.

3. RESULTS AND DISCUSSION

3.1. Proximate Nutrient Analysis of *S. pinnata* Fruit Pulp. Composition of the *S. pinnata* fruit pulp, obtained through proximate analysis, is mentioned in Table 1. Moisture content was primarily attributed to the water trapped in the pulp. Carbohydrates and crude fibers were identified as the other major components of *S. pinnata* fruit pulp. Ash and a small amount of crude protein were also found in *S. pinnata* fruit pulp. This proximate analysis was in close agreement with the previous report.[39]

Table 1. Proximate Nutrient Analysis of *S. Pinnata* Fruit Pulp

Component	Moisture	Carbohydrates	Ash	Crude fiber	Crude proteins
Quantity (%)	67.17	14.89	4.12	3.51	0.81

3.2. UV–Vis Spectroscopy. The UV–visible spectra of CS/PVA, CPPFE, CPAg–1, and CPAg–2 nanocomposite films are shown in Figure 3b. The characteristic peak appeared at 443 nm, associated with the surface plasmon resonance (SPR) of AgNPs,[23] which suggests the formation of AgNPs using the water extract of *S. pinnata* fruit pulp as a reducing agent. However, no such peak was observed for the pure CS/PVA film and *S. pinnata* fruit pulp extract. Hence, the results confirm that the peak at 443 nm corresponds to the AgNPs.

Packaging materials must protect food from sunlight. The light transmission, opacity, and transparency of the films are shown in Figure 3c,d. The UV light transmittance of SPPE-induced CPPFE film was reduced around 350–390 nm due to the presence of excess phenolic O–H groups, which undergo n → π^* transition.[40] The data (Figure 3) showed that the UV–vis light transparency of CPPFE was reduced by 7.45% compared with the neat CS/PVA film. When SPFPE and AgNPs were incorporated into the CS/PVA matrix, the light transparency was significantly reduced due to the influence of AgNPs. Among the CPAg nanocomposite films, CPAg-2 showed about 73. 83% lower UV–vis light transmittance than that of neat CS/PVA. Additionally, as seen in Figure 3d, the film opacity increased significantly due to the brownish color (Figure 3a) developed by AgNPs. The difference in the film transparency and opacity of the prepared films was due to the different amounts of fillers present in the film matrix, thickness, and visual appearance of the film samples.[41]

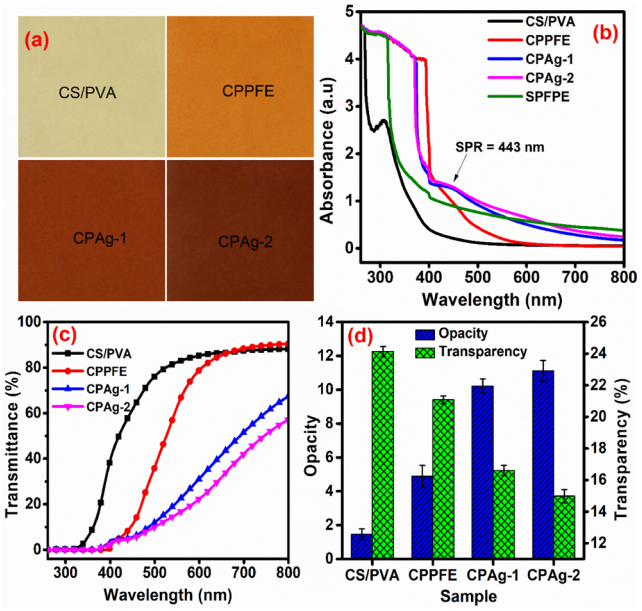

Figure 3. Digital images (a), UV absorbance (b), UV transmittance (c), and opacity at 500 nm and transparency at 600 nm of the prepared nanocomposite films (d).

3.3. SEM-EDS Analysis. The surface morphologies of the prepared CS/PVA, CPPFE, and CPAg nanocomposite films are shown in Figure 4. All the prepared films have homogeneous, crack-free surfaces. The incorporation of SPFPE into CS/PVA matrix led to the formation of marbling appearances on the film's surface due to the presence of plant phytochemicals that cause an increase in surface roughness, whereas bright spots appeared on the surface of CPAg-1 and CPAg-2 nanocomposite films. The appearance of the circular white patches on the CPAg nanocomposite films was due to the presence of agglomerated AgNPs, which led to an increase in surface roughness. It is evident from previous report that the incorporation of nanoparticles enhances the surface roughness of the films,[42] and the difference in the appearance of surface morphology from the previously reported results was due to slow or fast solvent evaporation and the purity of the polymer used for film preparation. In addition, it is evident from the EDS profile that the appearance of a silver peak in both CPAg-1 and CPAg-2 nanocomposite films confirms the presence of Ag particles.

3.4. XRD Analysis. X-ray diffraction patterns of CS/PVA, CPPFE, CPAg–1, and CPAg–2 nanocomposite films are shown in Figure 5. The CS/PVA and CPPFE films show two characteristic diffraction peaks at 2θ = 11.43° and 20.1°, attributed to the (020) and (110) planes, respectively.[43] Figure

https://doi.org/10.1021/acsfoodscitech.5c00238
ACS Food Sci. Technol. 2025, 5, 2430–2443

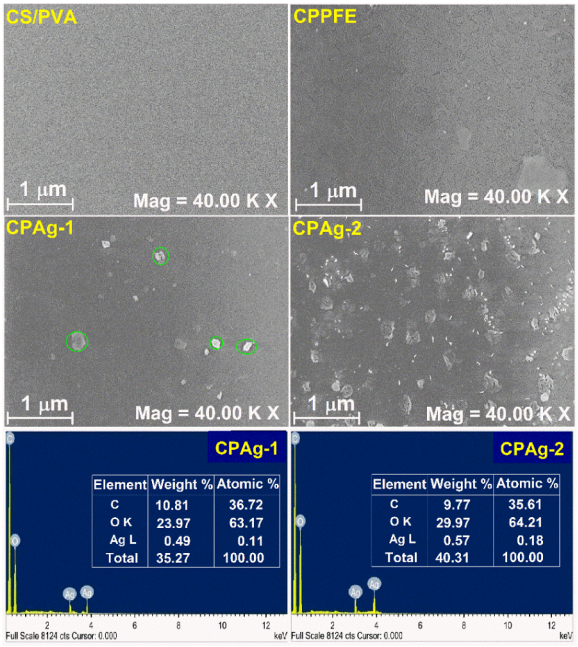

Figure 4. SEM-EDS profile of prepared nanocomposite films.

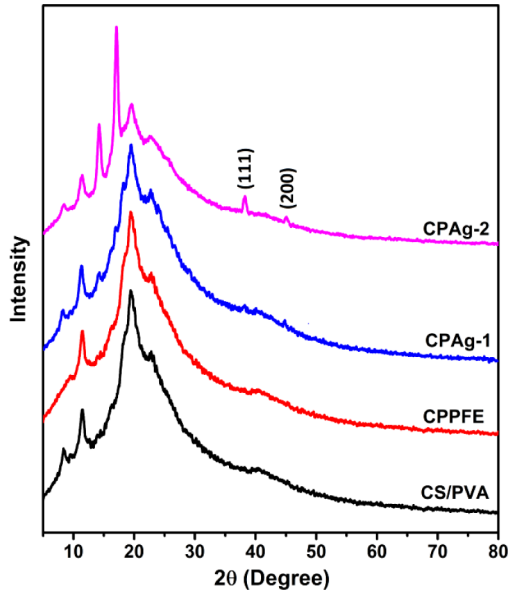

Figure 5. XRD pattern of prepared nanocomposite films.

5 depicts the appearance of two new diffraction peaks for the CPAg−1 and CPAg−2 nanocomposite films, which are assigned to the crystalline peaks of AgNPs corresponding to the (111) and (200) reflection planes, respectively.[44] The average crystallite sizes of AgNPs generated within the CS/PVA matrices were 11.3 and 16.7 nm, calculated by using the Debye-Scherrer equation, $C_S = K\lambda/\beta \cos \theta$ (where C_S− crystallite size, K− constant (0.94), λ− X−ray wavelength, β− FWHM of the diffraction line, and θ− diffraction angle).[45] In addition, the degree of crystallinity (X_C %) of the CS/PVA and CPPFE films was found to be 34.54 ± 0.98 and 32.17 ± 1.29, whereas the X_C % of the CPAg−1 and CPAg−2 films was 35.89 ± 1.21 and 38.88 ± 2.08, respectively. Due to the crystalline nature of the AgNPs present in the CS/PVA matrices, there is an increase in the degree of crystallinity of the nanocomposite films.

3.5. ATR−FT−IR Analysis. The bonding interactions between the CS, PVA, SPFPE, and AgNPs were investigated by ATR infrared spectroscopy, and the spectra of the prepared films are displayed in Figure 6. The neat CS/PVA film showed

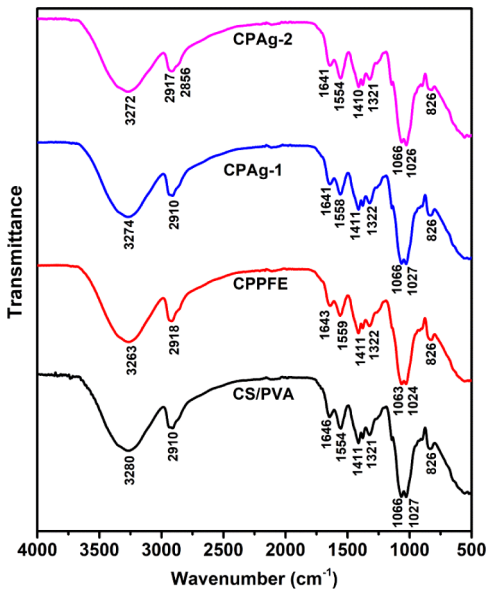

Figure 6. ATR−FT−IR spectra of prepared nanocomposite films.

a characteristic broad absorption band at 3280 cm^{-1}, which corresponds to the hydroxyl (O−H) and amine (−NH) stretching vibrations, and a band appearing at 2910 cm^{-1} was attributed to the C−H stretching of the methylene ($-CH_2$) group.[46] The absorption band that appeared at 1646 cm^{-1} was attributed to C═O stretching of the amide−I group, while the band appearing at 1554 cm^{-1} was associated with −NH bending of the amide−II group.[47] The bands that appeared at 1441 and 1321 cm^{-1} were assigned to O−H bending and C−H bending vibrations, respectively, whereas those around 1066 and 1027 cm^{-1} were assigned to the C−O−C stretching vibrations.[48] The absorption band at 826 cm^{-1} was ascribed to the C−H rocking of the CS and PVA polymeric chain.

With the incorporation of SPFPE into the CS/PVA matrix, the band positions corresponding to O−H stretching vibration and C−O−C stretching vibration were shifted to lower wavenumbers (Figure 6) suggesting intermolecular interactions as well as compatibility between the CS/PVA matrix and SPFPE. It is noteworthy that when the AgNPs were integrated into the polymer matrix, there was neither the appearance of new bands nor the disappearance of existing absorption bands related to the CS/PVA film. The band position corresponding to hydroxyl stretching and amine stretching vibrations was shifted to a lower wavenumber from 3280 to 3272 cm^{-1}, while the band related to C═O stretching was slightly shifted from 1646 to 1641 cm^{-1}. This slight shift in the peak position was due to the low chemical interaction between the *in situ* synthesized AgNPs and the CS/PVA matrix. Tao et al. (2017) reported that *in situ* generated AgNPs did not affect the inherent structure of the polymer matrix.[49]

3.6. Tensile Properties. Tensile properties of the prepared CS/PVA, CPPFE, and CPAg nanocomposite films were evaluated in terms of tensile strength (TS), Young's modulus

https://doi.org/10.1021/acsfoodscitech.5c00238
ACS Food Sci. Technol. 2025, 5, 2430−2443

(YM), and percent elongation at break (EAB) through stress–strain curves. The stress–strain curves are shown in Figure 7,

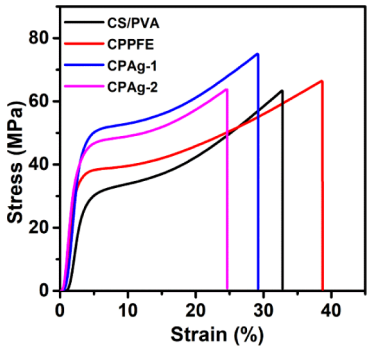

Figure 7. Stress–strain curves of the prepared nanocomposite films.

Table 2. Thickness, Tensile Strength, Percent Elongation at Break, and Young's Modulus of the Prepared Nanocomposite Films[a]

Sample	Thickness (μm)	TS (MPa)	EAB (%)	YM (GPa)
CS/PVA	81.21 ± 3.1^{c}	63.3 ± 0.8^{bc}	32.8 ± 1.1^{b}	1.1 ± 0.4^{c}
CPPFE	73.03 ± 4.0^{d}	66.5 ± 1.0^{b}	38.6 ± 0.9^{a}	1.5 ±0. 3^{b}
CPAg-1	94.14 ± 2.4^{b}	74.9 ± 1.3^{a}	29.1 ± 0.9^{c}	1.8 ± 0.4^{a}
CPAg-2	97.09 ± 3.2^{a}	63.7 ± 1.0^{b}	24.5 ± 1.0^{d}	1.8± 0.2^{a}

[a]Different letters within the same column represent significantly different values ($p \leq 0.05$), (mean ± SD, $n = 3$)

and the corresponding data are given in Table 2. The incorporation of SPFPE and AgNPs did not significantly affect the thickness of the CS/PVA film. According to the previous study, there were no significant ($p < 0.05$) changes in film thickness after integrating AgNPs.[50] As seen in Figure 7, the TS and EAB of neat CS/PVA without the incorporation of SPPE were 63.3 MPa and 32.8%, respectively. The TS and EAB of the CPPFE film were significantly ($p < 0.05$) enhanced by about ~4.97% and ~17.80%, respectively, compared to neat CS/PVA. The higher TS and YM can be utilized as indicators of the reliability of the film and its potential to endure mechanical stress when used in packaging.[51] On the other hand, when AgNPs along with SPFPE were incorporated into the CS/PVA film matrices, the highest TS (74.9 MPa) and YM (1.8 GPa) values were attained at 0.15 wt % of $AgNO_3$ (CPAg-1). Furthermore, the TS as well as YM values were reduced with an increase in the $AgNO_3$ content (0.45 wt%), but CPAg-2 still showed higher TS and YM values than the pure CS/PVA. However, the EAB values of CPAg-1 and CPAg-2 nanocomposite films were significantly reduced. At higher $AgNO_3$ concentrations, the breaking of the bonding interaction between the polymer matrices and nanofillers reduces TS and YM, while the presence of AgNPs in the film matrices restricts macromolecule movement and lowers the EAB of the films.[52]

3.7. Contact Angle (CA). The surface wettability behavior of the prepared nanocomposite films was evaluated through water contact angle measurements. Generally, film surfaces with a CA less than 65° and greater than 65° are considered to be hydrophilic and hydrophobic, respectively.[53] The contact angles of the prepared nanocomposite films are shown in Figure 8a. The neat CS/PVA had a CA of 81.5°, whereas the CA of the CPPFE film was found to be 68.4°. The decrease in the CA of the CPPFE film may be due to the hydrophilic properties of the phytochemicals present in the SPPE. The interaction between the nonpolar film surface and the polar solvent (distilled water) tends to increase the hydrophilicity.[54] On the other hand, the CA of CPAg-1 and CPAg-2 were found to be 75.5° and 86.5°, respectively, suggesting that the water resistance capacity of the film surface was significantly enhanced by the influence of in situ synthesized AgNPs. The significant enhancement in the CA of the nanocomposite films was attributed to the metallic character of the AgNPs present in the film matrix, which minimizes the spread rate of the water droplet on the film surface. Similar behavior of CA was observed for the AgNPs-incorporated biofilms.[50]

3.8. Moisture Absorption (MA) and Moisture Retention Capacity (MRC), Water Solubility (W_S), and Soil Burial Degradation (S_D) Test. The moisture absorption (MA) and moisture retention capacity (MRC) are among the most important properties of materials used in food packaging applications. The MA and MRC of the prepared films are summarized in Table 3. The neat CS/PVA has MA and MRC values of 14.49% and 87.34%, respectively. However, the incorporation of SPFPE into the solution caused a slight increase in the MA and a decrease in the MRC value. Further, the integration of CS/PVA films with *in situ*-generated AgNPs significantly enhanced the MA % and MRC % of the CPAg-1 and CPAg-2 due to the hydrophobic nature of the nanocomposite films (Figure 8a).

Water solubilities (W_S) of the prepared films are given in Table 3. The W_S of the nanocomposite films were found to be reduced upon the incorporation of AgNPs into the CS/PVA matrix. The insoluble metallic character of the AgNPs delayed the dissolution of the film matrix and enhanced water

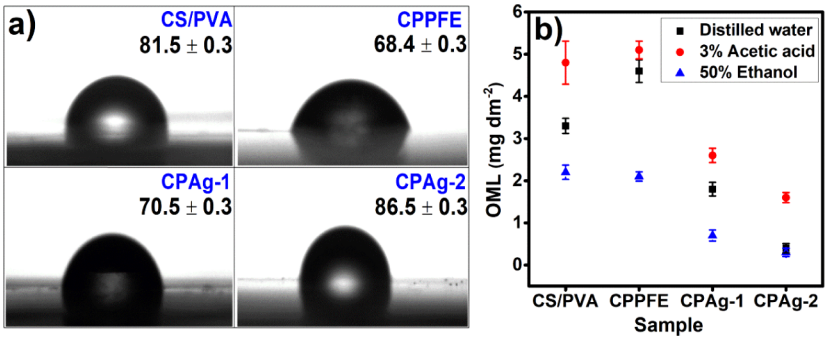

Figure 8. Water contact angle (a) and overall migration limit (b).

https://doi.org/10.1021/acsfoodscitech.5c00238
ACS Food Sci. Technol. 2025, 5, 2430–2443

Table 3. Moisture Absorption (MA), Water Solubility (W_S), Moisture Retention Capacity (MRC), Water Vapor Transmission Rate (WVTR) and Soil Degradability (S_D)[a]

Sample	MA (%)	MRC (%)	S_D (%)	W_S (%)	WVTR ($gm^{-2}·24h^{-1}$)
CS/PVA	14.49 ± 0.64[a]	87.34 ± 0.51[bc]	40.25 ± 0.86[b]	21.18 ± 1.07[b]	32.12 ± 0.14[b]
CPPFE	14.91 ± 0.37[a]	86.11 ± 0.29[bd]	46.16 ± 0.17[a]	24.27 ± 2.13[a]	34.24 ± 0.91[a]
CPAg−1	11.39 ± 0.21[b]	88.60 ± 0.37[b]	38.70 ± 1.07[c]	12.10 ± 0.89[c]	28.96 ± 0.82[c]
CPAg−2	8.95 ± 0.19[c]	91.04 ± 0.42[a]	37.35 ± 0.29[cd]	07.84 ± 0.17[d]	25.14 ± 1.07[d]

[a]Different letters within the same column represent significantly different values ($p \leq 0.05$). (Mean ± SD, $n = 3$)

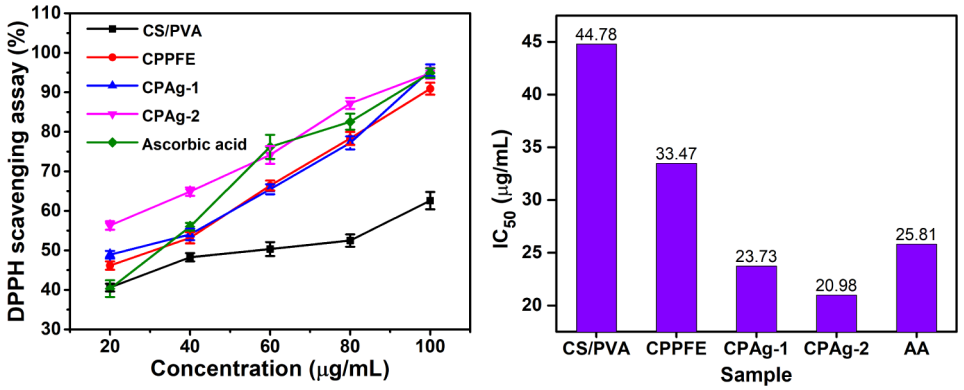

Figure 9. Antioxidant profiles of prepared nanocomposite films.

penetration, which caused a reduction in the solubility of the nanocomposite films. The incorporation of nanofillers reduces the solubility of the biofilms due to the ratio of dimensions and crystalline areas of fillers.[55] Also, the reduction in the water solubility of the biofilms is attributed to the minimal solubility of the NPs compared to the polymer chains, which leads to a reduction in the hydrophilicity of the polymer matrix.[56]

The degradation of plastic materials is a serious environmental problem. Usually, food packaging plastics are discarded after their use; hence, to reduce the environmental risks, the packaging films should be degradable under atmospheric conditions. The soil burial degradation (S_D) rate of CS/PVA, CPPFE, and CPAg nanocomposite films is mentioned in Table 3. The CS/PVA film exhibited an S_D of about 40.25%, while the CPPFE film showed a slightly higher S_D of 46.16%. On the other hand, the S_D of CPAg-1 and CPAg-2 was comparatively lower. The increase in the S_D of control films is probably due to the availability of organic elements such as C, O, and N, which serve as sources for microorganisms, and by the addition of water, microbes get activated and disrupt the polymer chains.[57] However, the antimicrobial property of the AgNPs present in the film matrix may inhibit the activation of the microbes, causing a delay in the degradation of the nanocomposite films.

3.9. Water Vapor Transmission Rate (WVTR). For the packaging materials, the water vapor transmission rate (WVTR) is one of the vital properties used to identify their suitability and effectiveness for the intended purpose.[58] It is important to note that the packaging film material should have a lower water vapor transmission rate to protect the food product from surrounding moisture vapors through its barrier properties. The WVTR data are summarized in Table 3. The CS/PVA and CPPFE films had higher WVTR values than the CPAg-1 and CPAg-2 nanocomposite films. The reduction in the WVTR of the AgNPs-incorporated films is attributed to the water-resistant capacity of the AgNPs, as well as an increase in the tortuous path network caused by AgNPs.[59] The nanoparticles integrated with the polymer matrices enhanced the binding ability between them, which led to an improvement in the water vapor barrier property of the CPAg films.

3.10. Overall Migration Limit (OML). Any material used for food packaging purposes must have a lower overall migration limit. According to the European Union (2011), the release of film constituents into the food simulants should be less than 10 mg dm^{-2}.[60] The OML profile is displayed in Figure 8b. The OML values of the CS/PVA film were found to be 4.8, 3.3, and 2.2 mg dm^{-2} against acetic acid, distilled water, and ethanol, respectively. In contrast, the CPPFE film exhibited higher OML values against acetic acid and distilled water compared to the pure CS/PVA film. This increase in the OML values was due to the solubility of CS and plant polyphenols in acetic acid and water, respectively. On the other hand, the OML of CPAg-1 and CPAg-2 nanocomposite films was significantly reduced against all three food simulants. This reduction in the OML of CPAg-1 and CPAg-2 was probably due to the presence of inert AgNPs, which form complex network structures that may restrict the release of film contents. Against the three food simulants, the OML values were highest in the acetic acid solution for all the prepared film samples, likely due to the rapid dissolution of CS in acidic pH.[61] Moreover, the OML values of the prepared films were below the permitted limit, indicating that these films possess promising properties for food packaging applications.

3.11. Antioxidant Activity. The food products rapidly undergo oxidation due to the surrounding environment. The proteins and lipids present in the food products eventually generate free radicals through an oxidation process. To overcome this, antioxidant packaging or substances were implemented to delay the oxidation process and prolong the product's shelf life. The antioxidant activity of the prepared films was determined through the DPPH free radical scavenging assay (%), and the efficiency of antioxidant films was expressed in terms of the half-maximal inhibitory concentration (IC_{50}) value. The antioxidant profiles of the

https://doi.org/10.1021/acsfoodscitech.5c00238
ACS Food Sci. Technol. 2025, 5, 2430−2443

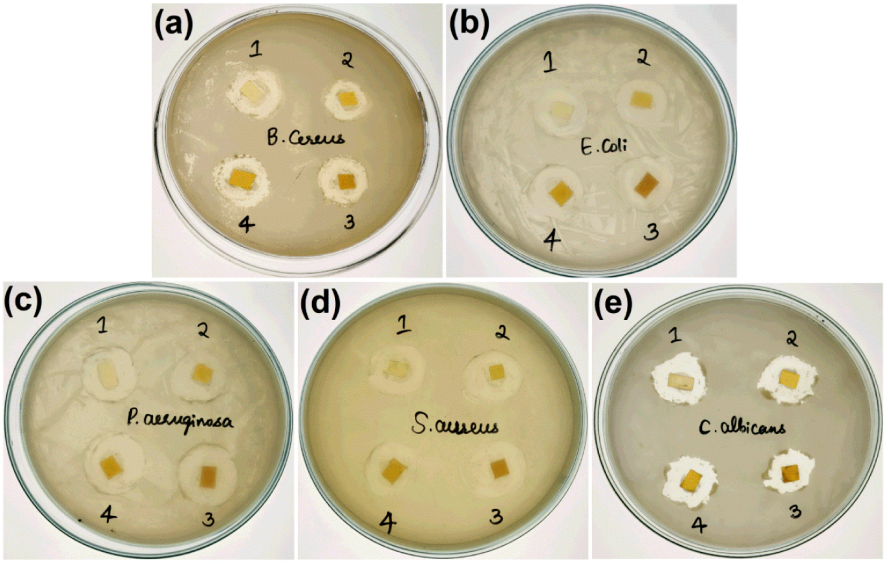

Figure 10. Microbial growth inhibition profile of prepared nanocomposite films against (**a**) *B. cereus*, (**b**) *E. coli*, (**c**) *P. aeruginosa*, (**d**) *S. aureus*, and (**e**) *C. albicans* (1-CS/PVA, 2-CPPFE, 3-CPAg-1, and 4-CPAg-2).

Table 4. Inhibition Zones of Prepared Nanocomposite Films Against Different Pathogens[a]

	Zone of Inhibition (mm)				
Sample	*B. cereus*	*E. coli*	*P. aeruginosa*	*S. aureus*	*C. albicans*
CS/PVA	16 ± 1.02^{b}	17 ± 0.97^{c}	16 ± 1.17^{d}	18 ± 1.05^{c}	18 ± 1.87^{c}
CPPFE	14 ± 0.91^{c}	17 ± 1.74^{c}	20 ± 1.21^{bc}	19 ± 0.82^{b}	19 ± 0.04^{c}
CPAg-1	19 ±1.19^{a}	18 ± 0.21^{b}	21 ± 0.16^{b}	19 ± 1.82^{b}	20 ± 0.79^{b}
CPAg-2	20 ±1.27^{a}	21 ± 1.27^{a}	22 ± 1.38^{a}	20 ± 1.49^{a}	23 ± 1.21^{a}

[a]Different letter within the same column represent significantly different values ($p \leq 0.05$). (Mean ± SD, $n = 3$).

CS/PVA, CPPFE, and CPAg nanocomposite films against DPPH radicals are listed in Figure 9. As expected, CS/PVA had low antioxidant capacity, whereas free radical scavenging was enhanced by the incorporation of SPPFE. The phytochemicals present in the extract readily stabilized the free radicals by donating a hydrogen atom. The DPPH radical scavenging activity of AgNPs and SPPFE-integrated CS/PVA films (CPAg-1 and CPAg-2) exhibited significant antioxidant activity. The strong free radical scavenging ability of AgNPs led to enhanced antioxidant activity.[62] As the film concentration increased, the scavenging assay also increased. This result suggests that the antioxidant activity was dose-dependent on DPPH free radicals. In addition, the IC_{50} value refers to the concentration of antioxidants needed to decrease the initial DPPH concentration by 50%; thus, the lower the IC_{50} value, the higher the antioxidant activity.[63] The IC_{50} values of the CPAg-1 and CPAg-2 nanocomposite films were found to be 23.73 and 20.98 mg/mL, respectively, which are lower than that of standard ascorbic acid. However, it is well known that samples with IC_{50} values of 10−50, 50−100, and greater than 100 μg/mL exhibited strong, moderate, and poor antioxidant efficiency, respectively. This enhanced antioxidant activity of the prepared nanocomposite films is attributed to the combined effect of plant polyphenols and AgNPs present in the CS/PVA matrices. Similar antioxidant behavior was observed for one-pot synthesized, tea polyphenolic-mediated, AgNPs-induced CS films.[64]

3.12. Antimicrobial Activity. To safeguard and extend the shelf life of foodstuffs, food packaging materials must be resistant to the growth of prevalent foodborne pathogens. The antibacterial inhibition profile of the prepared nanocomposite films is displayed in Figure 10 a−d and the corresponding inhibition zones are given in Table 4. As expected, the CS/PVA film exhibited lower antibacterial activity for all pathogens, which is attributed to the microbial resistant capacity of CS in a matrix. When SPFPE and AgNPs were introduced into the CS/PVA matrices, they enhanced the inhibition of tested bacterial growth. The film sample (CPAg-2), containing a higher concentration of AgNPs (0.45 wt %), showed greater antibacterial activity against *P. aeruginosa*, *E. coli*, and *S. aureus* followed by *B. cereus*. The difference in the cell wall membrane of each pathogen resulted in different antibacterial activity for the same film sample. On the other hand, the developed nanocomposite films demonstrated high antifungal activity against the most common yeast pathogen *C. albicans*. Similar to antibacterial activity, all film samples exhibited potential antifungal effects, with CPAg-2 showing the highest inhibition.

In both the antibacterial and antifungal activity profiles, the film samples act as both bacteriostatic as well as bactericidal agents, which means the film samples have the ability to prevent the microbial growth and damage pathogen DNA through membrane rupture, leading to the death of the pathogen. The key benefit of the bacteriostatic effect of the film is that it inhibits bacterial population growth over time while avoiding antimicrobial agent contamination from seeping into food products.[65] This mechanism of simultaneous bacteriostatic and bactericidal behavior was most likely due to the presence of AgNPs, which are considered as bacteriostatic and bactericidal agents,[66] and synergistic

https://doi.org/10.1021/acsfoodscitech.5c00238
ACS Food Sci. Technol. 2025, 5, 2430−2443

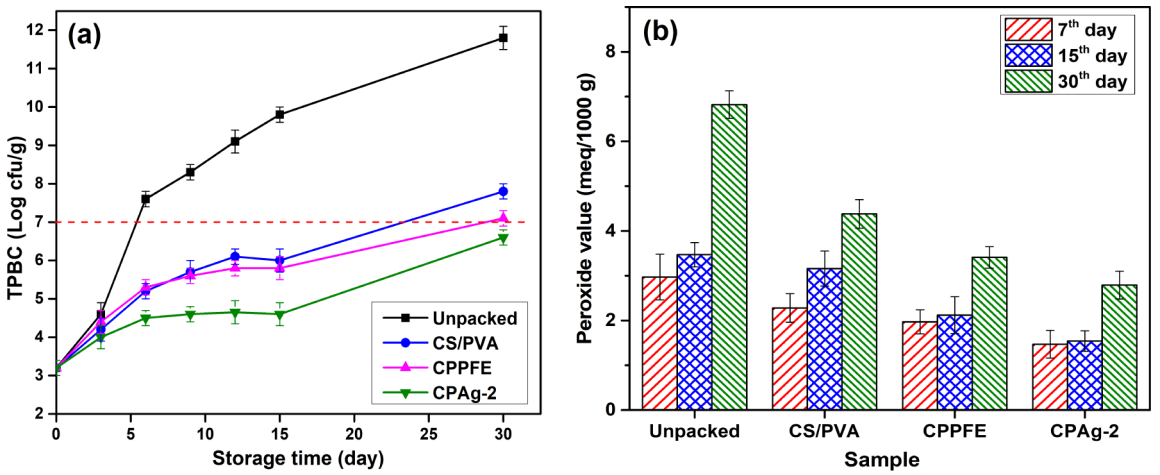

Figure 11. (a) Changes in the total psychrotrophic bacteria count (TPBC). (b) Changes in the peroxide value of lamb meat packaged with the prepared films over 30 days at 4 °C.

interactions between the hydroxyl groups in phytochemicals of SPPE present in CS/PVA matrices and the bacterial cell membrane. The silver ions released from the nanoparticles interact with the microbial cell membrane, leading to structural damage, disruption of metabolic processes, and ultimately, cell death.[67] Further, the presence of amino groups in the CS also contributes to the antibacterial effect by binding to negatively charged bacterial cell walls;[68] this may cause membrane disruption, resulting in cytoplasmic inclusion spillage and eventually cell death.[69] This combined action not only inhibits the growth of a wide spectrum of microorganisms but also prolongs the shelf life of packaged food products, particularly meat, by minimizing microbial spoilage.

3.13. Meat Packaging Efficacy. *3.13.1. Microbial Growth.* The cold storage is usually used for the preservation of meat products. However, psychrotrophic bacteria can grow under extremely cold conditions, which leads to contamination of the packed meat products. Hence, during cold storage, determining the total psychrotrophic bacteria count (TPBC) of packaged lamb meat provides valuable information about food hygiene and safety.[37] The change in the TPBC value of packed lamb meat during storage at 4 °C for 30 days is shown in Figure 11a. Initially, the TPBC value of the lamb meat was 3.2 log cfu/g, indicating that it was fresh and of good quality. The International Commission on Microbiological Specifications for Foods (ICMSF) has proposed the acceptable value of 7 log cfu/g for TPBC.[70] The TPBC value of unpacked lamb meat exceeded 7 log cfu/g within 6 days (i.e., 7.6 log cfu/g). On the other hand, the TPBC of lamb meat wrapped with CS/PVA, CPPFE, and CPAg-2 films gradually increased with an increase in storage time but remained below the permitted limit of 7 log cfu/g up to 15 days. The TPBC value of lamb meat wrapped with CS/PVA and CPPFE films increased by the 30th day and exceeded the acceptable value, whereas CPAg-2 reached 6.8 log cfu/g, which is below the standard permitted TPBC value.

By examining the total microbial count of the meat sample wrapped with prepared film samples, unpacked lamb meat retains its hygiene and quality for up to 6 days, whereas in the pristine CS/PVA and CPPFE packaging, it lasted for about 15 days, and in CPAg-2 film packaging, it lasted for 30 days at 4 °C. Various studies have shown that *S. pinnata* fruit pulp extract and AgNPs have the potential to inhibit the growth of foodborne pathogens.[71,72] For instance, the incorporation of AgNPs into the PVA-modified bacterial cellulose matrix retained the acceptable TPBC value of beef meat for up to 24 days when stored at 4 °C.[73] Further, Camo et al. (2008) claimed that the incorporation of the natural ingredient oregano, combined with a polystyrene coating, extended the shelf life of packed lamb meat up to 8−13 days at 4 °C.[74] Furthermore, Alizadeh-Sani et al. (2020) also demonstrated that packaging films consisting of whey protein/cellulose nanofiber matrices reinforced with TiO_2 nanoparticles and essential oil extended the shelf life of packed lamb meat up to 15 days while maintaining the TPBC value of 5−6 cfu/g.[75] Our results demonstrated that the prepared nanocomposite (CPAg-2) films are extremely effective in lamb meat preservation and shelf life extension at 4 °C, even in the absence of vacuum conditions, which may have substantial commercial implications. This lower TPBC value of lamb meat for up to 30 days is due to the combined effect of the bacteriostatic and bactericidal behaviors of the AgNPs and the antimicrobial efficiency of the SPPE and CS in the film matrix.

3.13.2. Estimation of Lipid Peroxidation. The lamb meat is attractive to consumers due to its tenderness and admirable fat content. It is important to maintain the fat content of lamb meat during storage and transport. A decrease in the fat content may lead to rancidity, rendering the meat unfit for consumption. In most cases, lipid peroxidation in meat samples is caused not only by reactive oxygen species but also by constant exposure to UV radiation.[76] During the lipid oxidation process, hydroperoxides are the major products; hence, measuring peroxide levels can help detect oxidative rancidity. The products obtained from the oxidation process cause harmful effects on human health due to the formation of carcinogenic and atherosclerotic agents.[77] Because of this issue, we estimated the total peroxide content during storage. Initially, the peroxide value of fresh lamb meat was found to be 1.27 mequiv/1000 g, indicating that the obtained lamb meat was in good condition and fresh. The unpacked meat sample showed a PV value of 2.97 mequiv/1000 g on the seventh day, while values of 2.28, 1.97, and 1.47 mequiv/1000 g were observed for CS/PVA, CPPFE, and CPAg-2 films, respectively (Figure 11b). As the storage time increased, the PV value of the unpacked meat sample drastically increased, attaining a maximum PV value of 6.82 mequiv/1000 g on the 30th day.

https://doi.org/10.1021/acsfoodscitech.5c00238
ACS Food Sci. Technol. 2025, 5, 2430−2443

However, the prepared films exhibited relatively low PV values (2−4.5 mequiv/1000 g). For instance, among the other samples, the meat wrapped with CPAg-2 nanocomposite film exhibited a relatively low PV value of 2.79 mequiv/1000 g, indicating that the lamb meat was in good condition (Figure 12).

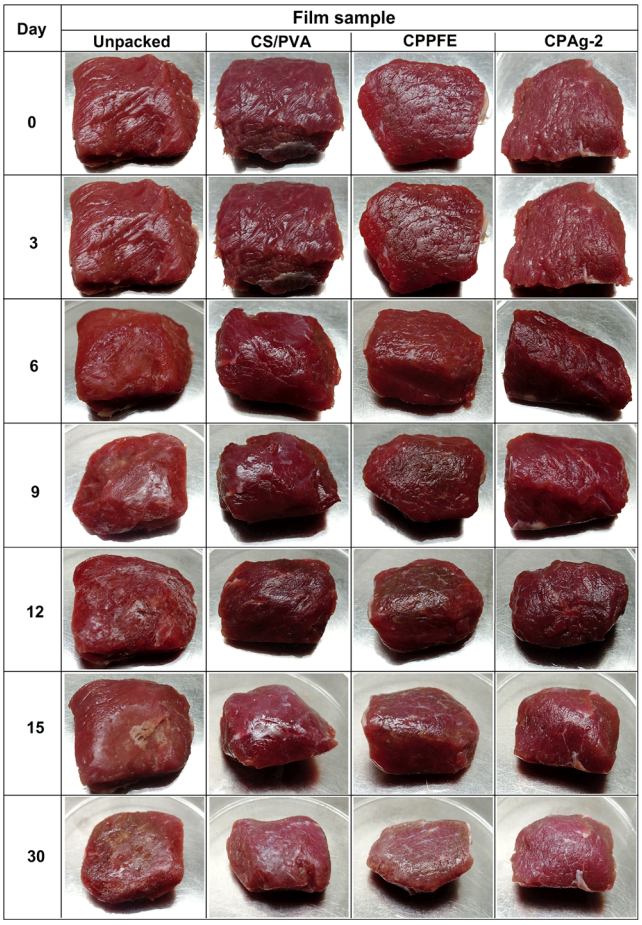

Figure 12. Digital images of lamb meat during storage at 4 °C.

Our findings proclaimed that the prepared CPAg nanocomposite films play a vital role in reducing the loss of fat content during storage and transportation. The lipid peroxidation mechanism of meat is mainly dependent on the active components present in the packaging systems and their storage conditions. The relatively low PV value of the CPAg-2 nanocomposite film is due to the strong antioxidant property of the film surface, attributed to the presence of AgNPs that hinder the formation of peroxides, and the active polyphenols present in the film matrix, which could delay the oxidation process of lipids and proteins. A previously reported study has demonstrated that the incorporation of natural polyphenols acts as a strong antioxidant agent to prevent the oxidation process.[78] Importantly, the prepared CPAg-2 nanocomposite film was able to reduce lamb meat lipid oxidation by 59.09% after 30 days. Beyond the preservation of lamb meat, the low cost, degradability, antimicrobial, antioxidant, and high UV-resistant properties of the CPAg nanocomposite film suggest its potential for broader applications. These might include packaging for dairy, marine, poultry, and other perishable foods.

Overall, these results underscore the successful development of an eco-friendly bionanocomposite film based on CS/PVA integrated with AgNPs, synthesized using *S. pinnata* fruit pulp extract through a facile one-pot approach. The SEM micrographs suggest that the incorporation of Ag at concentrations of 0.15 and 0.45 wt % appeared to be crack-free and homogeneous, which reduced the polymer free volume and led to an increase in mechanical strength of approximately 16.65%. Further, the presence of AgNPs in the film matrix significantly enhanced the UV−vis light-blocking ability, surface wettability, and WVTR, whereas the soil burial degradation of the CPAg nanocomposite films was found to be ∼37.5% over 15 days. In addition, the prepared CPAg nanocomposite films (0.45 wt %) had a significantly lower overall migration value than the permitted limit of 10 mg·dm^{-2} and the antioxidant property against DPPH free radicals was enhanced by 53.84% (CPAg-2) compared to the pristine CS/PVA film. Furthermore, CPAg nanocomposite films displayed potential antibacterial and antifungal activities against common Gram-positive bacteria (*Staphylococcus aureus*, *Bacillus cereus*) and Gram-negative bacteria (*E. coli* and *P. aeruginosa*), as well as the fungus *C. albicans*. Notably, the CPAg-2 nanocomposite film was able to extend the shelf life of lamb meat up to 30 days when stored at 4 °C. Based on the above results, the prepared nanocomposite films are considered to be a promising material for meat packaging applications. These multifunctional films are well-aligned with current market trends, particularly with the growing demand for biodegradable packaging solutions worldwide. These bionanocomposite films have economic potential in the future of the packaging industry, which is highlighted by the increased emphasis on sustainability, further supported by changes in environmental regulations and consumer awareness.

■ ASSOCIATED CONTENT

Supporting Information

The Supporting Information is available free of charge at https://pubs.acs.org/doi/10.1021/acsfoodscitech.5c00238.

The supporting file contains the film composition in Table S1 (PDF)

■ AUTHOR INFORMATION

Corresponding Authors

Ravindra B. Chougale − *P.G. Department of Chemistry, Karnatak University, Dharwad 580 003, India*; Email: ravindrabc@kud.ac.in

Tilak Gasti − *Department of Chemistry, Faculty of Sciences, Khaja Bandanawaz University, Kalaburagi 585 104, India; P.G. Department of Chemistry, Karnatak University, Dharwad 580 003, India*; orcid.org/0000-0002-0737-3032; Email: tilak.chem86@gmail.com, tilakgasti@kbn.university

Authors

Shruti Dixit − *Department of Microbiology, Gulbarga University, Kalaburagi 585 106, India*; orcid.org/0000-0001-6581-5233

Lokesh A. Shastri − *P.G. Department of Chemistry, Karnatak University, Dharwad 580 003, India*

Bhagyavana S. Mudigoudra − *Department of Computer Science, Maharani Cluster University, Bangalore 560 001, India*

https://doi.org/10.1021/acsfoodscitech.5c00238
ACS Food Sci. Technol. 2025, 5, 2430−2443

Saraswati P. Masti − *Department of Chemistry, Karnatak Science College, Dharwad 580 001, India;* orcid.org/0000-0001-7476-0545

Complete contact information is available at: https://pubs.acs.org/10.1021/acsfoodscitech.5c00238

Author Contributions

T.G.: conceptualization, methodology, data curation, formal analysis, resources, investigation, corresponding author, and writing—original draft. S.D.: methodology, data curation, formal analysis, investigation, and writing—original draft. L.A.S. and S.P.M.: conceptualization, writing—review and editing, and supervision. B.S.M.: software, data curation, formal analysis, and writing—original draft. R.B.C.: conceptualization, writing—review and editing, supervision, and corresponding author.

Funding

This work received no specific support from public, private, or nonprofit funding bodies.

Notes

The authors declare no competing financial interest.

■ ACKNOWLEDGMENTS

The authors acknowledge the University Scientific Instrument Centre (USIC), DST-SAIF, and the DST-PURSE-Phase-II program [Grant No.SR/PURSE PHASE 2/13 (G)], Karnatak University, Dharwad, for providing the necessary characterization facilities. Authors also acknowledge Khaja Bandanawaz University for providing essential facilities. The authors are thankful to Dr. M.A. Mujeeb, Assistant Professor, Department of Biotechnology, Khaja Bandanawaz University, Kalaburagi, for his assistance in editing the language and improving the clarity of the manuscript.

■ REFERENCES

(1) Fao. *The State of Food and Agriculture 2019: moving Forward on Food Loss and Waste Reduction*; FAO, 2019.
(2) Uhlig, E.; Sadzik, A.; Strenger, M.; Schneider, A.-M.; Schmid, M. Food Wastage along the Global Food Supply Chain and the Impact of Food Packaging. *J. Consum. Prot. Food Saf.* **2025**, *20* (1), 5−17.
(3) Achari, D. D.; Kouser, S.; Gasti, T.; Dixit, S. Biodegradable Polymer Blends in Food Packaging and Preservation. In *Sustainable Materials for Food Packaging and Preservation*, Ghosh, T.; Priyadarshi, R.; Roy, S., Eds.; Elsevier, 2025, pp. 171−197. .
(4) Al-Tayyar, N. A.; Youssef, A. M.; Al-Hindi, R. R. Antimicrobial Packaging Efficiency of ZnO-SiO2 Nanocomposites Infused into PVA/CS Film for Enhancing the Shelf Life of Food Products. *Food Packag. Shelf Life* **2020**, *25* (April), 100523.
(5) Kong, P.; Rosnan, S. M.; Enomae, T. Carboxymethyl Cellulose−Chitosan Edible Films for Food Packaging: A Review of Recent Advances. *Carbohydr. Polym.* **2024**, *346*, 122612.
(6) Rodríguez-Núñez, J. R.; Madera-Santana, T. J.; Sánchez-Machado, D. I.; López-Cervantes, J.; Soto Valdez, H. Chitosan/Hydrophilic Plasticizer-Based Films: Preparation, Physicochemical and Antimicrobial Properties. *J. Polym. Environ.* **2014**, *22* (1), 41−51.
(7) Narasagoudr, S. S.; Hegde, V. G.; Vanjeri, V. N.; Chougale, R. B.; Masti, S. P. Ethyl Vanillin Incorporated Chitosan/Poly(Vinyl Alcohol) Active Films for Food Packaging Applications. *Carbohydr. Polym.* **2020**, *236*, 116049.
(8) Suganthi, S.; Vignesh, S.; Kalyana Sundar, J.; Raj, V. Fabrication of PVA Polymer Films with Improved Antibacterial Activity by Fine-Tuning via Organic Acids for Food Packaging Applications. *Appl. Water Sci* **2020**, *10* (4), 100.
(9) Dhaka, A.; Chand Mali, S.; Sharma, S.; Trivedi, R. A Review on Biological Synthesis of Silver Nanoparticles and Their Potential Applications. *Results Chem* **2023**, *6*, 101108.
(10) Chaudhary, P.; Fatima, F.; Kumar, A. Relevance of Nanomaterials in Food Packaging and Its Advanced Future Prospects. *J. Inorg. Organomet. Polym. Mater.* **2020**, *30* (12), 5180−5192.
(11) Abbas, A.; Amin, H. M. A.; Akhtar, M.; Hussain, M. A.; Batchelor-McAuley, C.; Compton, R. G. Eco-Friendly Polymer Succinate Capping on Silver Nano-Particles for Enhanced Stability: A UV-Vis and Electrochemical Particle Impact Study. *Chemia Naissensis* **2020**, *3* (1), 50−70.
(12) Anees Ahmad, S.; Sachi Das, S.; Khatoon, A.; Tahir Ansari, M.; Afzal, M.; Saquib Hasnain, M.; Kumar Nayak, A. Bactericidal Activity of Silver Nanoparticles: A Mechanistic Review. *Mater. Sci. Energy Technol.* **2020**, *3*, 756−769.
(13) Ullah, S.; Khalid, R.; Rehman, M. F.; Irfan, M. I.; Abbas, A.; Alhoshani, A.; Anwar, F.; Amin, H. M. A. Biosynthesis of Phyto-Functionalized Silver Nanoparticles Using Olive Fruit Extract and Evaluation of Their Antibacterial and Antioxidant Properties. *Front. Chem.* **2023**, *11*, 1202252.
(14) Assad, N.; Naeem-Ul-Hassan, M.; Ajaz Hussain, M.; Abbas, A.; Sher, M.; Muhammad, G.; Assad, Y.; Farid-Ul-Haq, M. Diffused Sunlight Assisted Green Synthesis of Silver Nanoparticles Using *Cotoneaster Nummularia* Polar Extract for Antimicrobial and Wound Healing Applications. *Nat. Prod. Res.* **2025**, *39* (8), 2203−2217.
(15) Mao, L.; Wang, C.; Yao, J.; Lin, Y.; Liao, X.; Lu, J. Design and Fabrication of Anthocyanin Functionalized Layered Clay/Poly(Vinyl Alcohol) Coatings on Poly(Lactic Acid) Film for Active Food Packaging. *Food Packag. Shelf Life* **2023**, *35*, 101007.
(16) Wen, Y.; Liu, J.; Jiang, L.; Zhu, Z.; He, S.; He, S.; Shao, W. Development of Intelligent/Active Food Packaging Film Based on TEMPO-Oxidized Bacterial Cellulose Containing Thymol and Anthocyanin-Rich Purple Potato Extract for Shelf Life Extension of Shrimp. *Food Packag. Shelf Life* **2021**, *29*, 100709.
(17) Kanatt, S. R. Development of Active/Intelligent Food Packaging Film Containing Amaranthus Leaf Extract for Shelf Life Extension of Chicken/Fish during Chilled Storage. *Food Packag. Shelf Life* **2020**, *24*, 100506.
(18) Hazra, B.; Biswas, S.; Mandal, N. Antioxidant and Free Radical Scavenging Activity of Spondias Pinnata. *BMC Complement Altern. Med.* **2008**, *8* (1), 63.
(19) Gupta, V. K.; Roy, A.; Nigam, V. K.; Mukherjee, K. Antimicrobial Activity of Spondias Pinnata Resin. *J. Med. Plants Res.* **2010**, *4* (16), 1656−1661.
(20) Patathananone, S.; Daduang, J.; Koraneekij, A.; Li, C.-Y. Tyrosinase Inhibitory Effect, Antioxidant and Anticancer Activities of Bioactive Compounds in Ripe Hog Plum (Spondias Pinnata) Fruit Extracts. *Orient. J. Chem.* **2019**, *35* (3), 916−926.
(21) Bora, N. S.; Kakoti, B. B.; Gogoi, B.; Goswami, A. K. Ethno-Medicinal Claims, Phytochemistry and Pharmacology of Spondias Pinnata: A Review. *Int. J. Pharm. Sci. Res.* **2014**, *5* (4), 1138−1145.
(22) Gasti, T.; Dixit, S.; Chougale, R. B.; Masti, S. P. Fabrication of Novel Gallic Acid Functionalized Chitosan/Pullulan Active Bio-Films for the Preservation and Shelf-Life Extension of Green Chillies. *Sustainable Food Technol.* **2023**, *1* (3), 390−403.
(23) Nwabor, O. F.; Singh, S.; Paosen, S.; Vongkamjan, K.; Voravuthikunchai, S. P. Enhancement of Food Shelf Life with Polyvinyl Alcohol-Chitosan Nanocomposite Films from Bioactive Eucalyptus Leaf Extracts. *Food Biosci.* **2020**, *36* (April), 100609.
(24) Ragab, H. M.; Diab, N. S.; Obeidat, S. T.; Alghamdi, A. M.; Khaled, A. M.; Farea, M. O.; Morsi, M. A. Improving the Optical, Thermal, Mechanical, Electrical Properties and Antibacterial Activity of PVA-Chitosan by Biosynthesized Ag Nanoparticles: Eco-Friendly Nanocomposites for Food Packaging Applications. *Int. J. Biol. Macromol.* **2024**, *264*, 130668.
(25) Tran, N. T. Aloe Vera-Synthesized Ag Nanoparticles Loaded on PVA/Chitosan as Biodegradable and Antibacterial Film for Food Storage. *Mater. Res. Express* **2024**, *11* (8), 085010.

(26) Guo, Q.; Ghadiri, R.; Weigel, T.; Aumann, A.; Gurevich, E.; Esen, C.; Medenbach, O.; Cheng, W.; Chichkov, B.; Ostendorf, A. Comparison of in Situ and Ex Situ Methods for Synthesis of Two-Photon Polymerization Polymer Nanocomposites. *Polymers* **2014**, *6* (7), 2037−2050.
(27) Zare, Y. Study of Nanoparticles Aggregation/Agglomeration in Polymer Particulate Nanocomposites by Mechanical Properties. *Composites, Part A* **2016**, *84*, 158−164.
(28) Kumar, S.; Shukla, A.; Baul, P. P.; Mitra, A.; Halder, D. Biodegradable Hybrid Nanocomposites of Chitosan/Gelatin and Silver Nanoparticles for Active Food Packaging Applications. *Food Packag. Shelf Life* **2018**, *16*, 178−184.
(29) Garzón, G. A.; Narváez-Cuenca, C.-E.; Kopec, R. E.; Barry, A. M.; Riedl, K. M.; Schwartz, S. J. Determination of Carotenoids, Total Phenolic Content, and Antioxidant Activity of Arazá (Eugenia Stipitata McVaugh), an Amazonian Fruit. *J. Agric. Food Chem.* **2012**, *60* (18), 4709−4717.
(30) Conklin-Brittain, N. L.; Dierenfeld, E. S.; Wrangham, R. W.; Norconk, M.; Silver, S. C. Chemical Protein Analysis: A Comparison of Kjeldahl Crude Protein and Total Ninhydrin Protein from Wild, Tropical Vegetation. *J. Chem. Ecol.* **1999**, *25* (12), 2601−2622.
(31) Rambabu, K.; Bharath, G.; Banat, F.; Show, P. L.; Cocoletzi, H. H. Mango Leaf Extract Incorporated Chitosan Antioxidant Film for Active Food Packaging. *Int. J. Biol. Macromol.* **2019**, *126*, 1234−1243.
(32) Gasti, T.; Dixit, S. Development of Poly (Vinyl Alcohol)/Nano-Clay/Ipomoea Cairica Anthocyanin Based Halochromic Smart Films for Freshness Monitoring of Lamb Meat. *Food Biosci.* **2024**, *60*, 104441.
(33) Zimet, P.; Mombrú, Á. W.; Mombrú, D.; Castro, A.; Villanueva, J. P.; Pardo, H.; Rufo, C. Physico-Chemical and Antilisterial Properties of Nisin-Incorporated Chitosan/Carboxymethyl Chitosan Films. *Carbohydr. Polym.* **2019**, *219* (April), 334−343.
(34) Gasti, T.; Dixit, S.; Sataraddi, S. P.; Hiremani, V. D.; Masti, S. P.; Chougale, R. B.; Malabadi, R. B. Physicochemical and Biological Evaluation of Different Extracts of Edible Solanum Nigrum L. Leaves Incorporated Chitosan/Poly (Vinyl Alcohol) Composite Films. *J. Polym. Environ.* **2020**, *28* (11), 2918−2930.
(35) Goudar, N.; Vanjeri, V. N.; Dixit, S.; Hiremani, V.; Sataraddi, S.; Gasti, T.; Vootla, S. K.; Masti, S. P.; Chougale, R. B. Evaluation of Multifunctional Properties of Gallic Acid Crosslinked Poly (Vinyl Alcohol)/Tragacanth Gum Blend Films for Food Packaging Applications. *Int. J. Biol. Macromol.* **2020**, *158*, 139−149.
(36) Hajji, S.; Salem, R. B. S. B.; Hamdi, M.; Jellouli, K.; Ayadi, W.; Nasri, M.; Boufi, S. Nanocomposite films based on chitosan−poly(vinyl alcohol) and silver nanoparticles with high antibacterial and antioxidant activities. *Process Saf. Environ. Prot.* **2017**, *111*, 112−121.
(37) Priyadarshi, R.; Kim, S.-M.; Rhim, J.-W. Carboxymethyl Cellulose-Based Multifunctional Film Combined with Zinc Oxide Nanoparticles and Grape Seed Extract for the Preservation of High-Fat Meat Products. *Sustainable Mater. Technol.* **2021**, *29* (March), No. e00325.
(38) Hornero-Méndez, D.; Pérez-Gálvez, A.; Mínguez-Mosquera, M. I. A Rapid Spectrophotometric Method for the Determination of Peroxide Value in Food Lipids with High Carotenoid Content. *J. Am. Oil Chem. Soc.* **2001**, *78* (11), 1151−1155.
(39) Andola, H. C.; Purohit, V. K. Nutritive and Mineral Value of Ripe Fruits Evaluation of Nutritive and Mineral Value in Ripe Fruits of Spondias Pinnata from Two Location of Western Himalaya, India. *Med. Plants - Int. J. Phytomed.* **2010**, *2* (3), 233.
(40) Narasagoudr, S. S.; Hegde, V. G.; Chougale, R. B.; Masti, S. P.; Vootla, S.; Malabadi, R. B. Physico-Chemical and Functional Properties of Rutin Induced Chitosan/Poly (Vinyl Alcohol) Bioactive Films for Food Packaging Applications. *Food Hydrocoll* **2020**, *109*, 106096.
(41) Li, J.; Miao, J.; Wu, J.; Chen, S.; Zhang, Q. Food Hydrocolloids Preparation and Characterization of Active Gelatin-Based Fi Lms Incorporated with Natural Antioxidants. *Food Hydrocoll* **2014**, *37*, 166−173.
(42) Wu, C.; Li, Y.; Du, Y.; Wang, L.; Tong, C.; Hu, Y.; Pang, J.; Yan, Z. Preparation and Characterization of Konjac Glucomannan-Based Bionanocomposite Film for Active Food Packaging. *Food Hydrocoll* **2019**, *89*, 682−690.
(43) Jbeli, A.; Hamden, Z.; Bouattour, S.; Ferraria, A. M.; Conceição, D. S.; Ferreira, L. F. V.; Chehimi, M. M.; Do Rego, A. M. B.; Rei Vilar, M.; Boufi, S. Chitosan-Ag-TiO2 Films: An Effective Photocatalyst under Visible Light. *Carbohydr. Polym.* **2018**, *199*, 31−40.
(44) Venkatesham, M.; Ayodhya, D.; Madhusudhan, A.; Veera Babu, N.; Veerabhadram, G. A Novel Green One-Step Synthesis of Silver Nanoparticles Using Chitosan: Catalytic Activity and Antimicrobial Studies. *Appl. Nanosci.* **2014**, *4* (1), 113−119.
(45) Krstić, J.; Spasojević, J.; Radosavljević, A.; Šiljegovć, M.; Kačarević-Popović, Z. Optical and Structural Properties of Radiolytically in Situ Synthesized Silver Nanoparticles Stabilized by Chitosan/Poly(Vinyl Alcohol) Blends. *Radiat. Phys. Chem.* **2014**, *96*, 158−166.
(46) Gasti, T.; Hiremani, V. D.; Sataraddi, S. P.; Vanjeri, V. N.; Goudar, N.; Masti, S. P.; Chougale, R. B.; Malabadi, R. B. UV Screening, Swelling and in-Vitro Cytotoxicity Study of Novel Chitosan/Poly (1-Vinylpyrrolidone-Co-Vinyl Acetate) Blend Films. *Chem. Data Coll.* **2021**, *33*, 100684.
(47) Shankar, S.; Rhim, J. W. Preparation of Sulfur Nanoparticle-Incorporated Antimicrobial Chitosan Films. *Food Hydrocoll* **2018**, *82*, 116−123.
(48) Tomadoni, B.; Ponce, A.; Pereda, M.; Ansorena, M. R. Vanillin as a Natural Cross-Linking Agent in Chitosan-Based Films: Optimizing Formulation by Response Surface Methodology. *Polym. Test.* **2019**, *78* (June), 105935.
(49) Tao, G.; Cai, R.; Wang, Y.; Song, K.; Guo, P.; Zhao, P.; Zuo, H. Biosynthesis and Characterization of AgNPs−Silk/PVA Film for Potential Packaging Application. *Materials* **2017**, *10* (6), 667.
(50) Rhim, J. W.; Wang, L. F.; Hong, S. I. Preparation and Characterization of Agar/Silver Nanoparticles Composite Films with Antimicrobial Activity. *Food Hydrocoll* **2013**, *33* (2), 327−335.
(51) Kanmani, P.; Rhim, J.-W. Physical, Mechanical and Antimicrobial Properties of Gelatin Based Active Nanocomposite Films Containing AgNPs and Nanoclay. *Food Hydrocoll* **2014**, *35*, 644−652.
(52) Sarwar, M. S.; Niazi, M. B. K.; Jahan, Z.; Ahmad, T.; Hussain, A. Preparation and Characterization of PVA/Nanocellulose/Ag Nanocomposite Films for Antimicrobial Food Packaging. *Carbohydr. Polym.* **2018**, *184*, 453−464.
(53) Vogler, E. A. Structure and Reactivity of Water at Biomaterial Surfaces. *Adv. Colloid Interface Sci.* **1998**, *74* (1−3), 69−117.
(54) Ramírez, C.; Gallegos, I.; Ihl, M.; Bifani, V. Study of Contact Angle, Wettability and Water Vapor Permeability in Carboxymethylcellulose (CMC) Based Film with Murta Leaves (Ugni Molinae Turcz) Extract. *J. Food Eng.* **2012**, *109* (3), 424−429.
(55) Jamróz, E.; Kulawik, P.; Kopel, P. The Effect of Nanofillers on the Functional Properties of Biopolymer-Based Films: A Review. *Polymers* **2019**, *11* (4), 1−42.
(56) Oleyaei, S. A.; Zahedi, Y.; Ghanbarzadeh, B.; Moayedi, A. A. Modification of Physicochemical and Thermal Properties of Starch Films by Incorporation of TiO2 Nanoparticles. *Int. J. Biol. Macromol.* **2016**, *89*, 256−264.
(57) Kaya, M.; Khadem, S.; Cakmak, Y. S.; Mujtaba, M.; Ilk, S.; Akyuz, L.; Salaberria, A. M.; Labidi, J.; Abdulqadir, A. H.; Deligöz, E. Antioxidative and Antimicrobial Edible Chitosan Films Blended with Stem, Leaf and Seed Extracts of Pistacia Terebinthus for Active Food Packaging. *RSC Adv.* **2018**, *8* (8), 3941−3950.
(58) Turan, D. Water Vapor Transport Properties of Polyurethane Films for Packaging of Respiring Foods. *Food Eng. Rev.* **2021**, *13* (1), 54−65.
(59) Yu, J.; Yang, J.; Liu, B.; Ma, X. Preparation and Characterization of Glycerol Plasticized-Pea Starch/ZnO−Carboxymethylcellulose Sodium Nanocomposites. *Bioresour. Technol.* **2009**, *100* (11), 2832−2841.

https://doi.org/10.1021/acsfoodscitech.5c00238
ACS Food Sci. Technol. 2025, 5, 2430−2443

(60) European Commission *European Union Commission Regulation (EU) No 10/2011 of 14 January 2011. Official Journal Of The European UnionSpecial Ed*, 2011, 1−89.
(61) Priyadarshi, R.; Rhim, J.-W. Chitosan-Based Biodegradable Functional Films for Food Packaging Applications. *Innovative Food Sci. Emerging Technol.* **2020**, *62* (April), 102346.
(62) Ajdary, M.; Negahdary, M.; Chelongar, R.; Zadeh, S. The Antioxidant Effects of Silver, Gold, and Zinc Oxide Nanoparticles on Male Mice in in Vivo Condition. *Adv. Biomed. Res.* **2015**, *4* (1), 69.
(63) Rivero-Cruz, J. F.; Granados-Pineda, J.; Pedraza-Chaverri, J.; Pérez-Rojas, J. M.; Kumar-Passari, A.; Diaz-Ruiz, G.; Rivero-Cruz, B. E. Phytochemical Constituents, Antioxidant, Cytotoxic, and Antimicrobial Activities of the Ethanolic Extract of Mexican Brown Propolis. *Antioxidants* **2020**, *9* (1), 70.
(64) Zhang, W.; Jiang, W. Antioxidant and Antibacterial Chitosan Film with Tea Polyphenols-Mediated Green Synthesis Silver Nanoparticle via a Novel One-Pot Method. *Int. J. Biol. Macromol.* **2020**, *155*, 1252−1261.
(65) Biswas, M. C.; Tiimob, B. J.; Abdela, W.; Jeelani, S.; Rangari, V. K. Nano Silica-Carbon-Silver Ternary Hybrid Induced Antimicrobial Composite Films for Food Packaging Application. *Food Packag. Shelf Life* **2019**, *19*, 104−113.
(66) Dakal, T. C.; Kumar, A.; Majumdar, R. S.; Yadav, V. Mechanistic Basis of Antimicrobial Actions of Silver Nanoparticles. *Front. Microbiol.* **2016**, *7* (NOV), 1−17.
(67) Zhou, P.; Xia, Z.; Qi, C.; He, M.; Yu, T.; Shi, L. Construction of Chitosan/Ag Nanocomposite Sponges and Their Properties. *Int. J. Biol. Macromol.* **2021**, *192*, 272−277.
(68) He, M.; Huang, Y.; Wang, J.; Chen, Z.; Xie, J.; Cui, Z.; Xu, D.; Zhang, X.; Yao, W. Advances in Polysaccharide-Based Antibacterial Materials. *Int. J. Biol. Macromol.* **2025**, *308*, 142598.
(69) Surendhiran, D.; Li, C.; Cui, H.; Lin, L. Fabrication of High Stability Active Nanofibers Encapsulated with Pomegranate Peel Extract Using Chitosan/PEO for Meat Preservation. *Food Packag. Shelf Life* **2020**, *23*, 100439.
(70) Alizadeh-Sani, M.; Mohammadian, E.; McClements, D. J. Eco-Friendly Active Packaging Consisting of Nanostructured Biopolymer Matrix Reinforced with TiO2 and Essential Oil: Application for Preservation of Refrigerated Meat. *Food Chem.* **2020**, *322* (April), 126782.
(71) Satpathy, G.; Tyagi, Y. K.; Gupta, R. K. Preliminary Evaluation of Nutraceutical and Therapeutic Potential of Raw Spondias Pinnata K., an Exotic Fruit of India. *Food Res. Int.* **2011**, *44* (7), 2076−2087.
(72) Gudimalla, A.; Jose, J.; Varghese, R. J.; Thomas, S. Green Synthesis of Silver Nanoparticles Using Nymphae Odorata Extract Incorporated Films and Antimicrobial Activity. *J. Polym. Environ.* **2020**, *29*, 0123456789.
(73) Wang, W.; Yu, Z.; Alsammarraie, F. K.; Kong, F.; Lin, M.; Mustapha, A. Properties and Antimicrobial Activity of Polyvinyl Alcohol-Modified Bacterial Nanocellulose Packaging Films Incorporated with Silver Nanoparticles. *Food Hydrocoll* **2020**, *100*, 105411.
(74) Camo, J.; Beltrán, J. A.; Roncalés, P. Extension of the Display Life of Lamb with an Antioxidant Active Packaging. *Meat Sci.* **2008**, *80* (4), 1086−1091.
(75) Alizadeh-Sani, M.; Mohammadian, E.; McClements, D. J. Eco-Friendly Active Packaging Consisting of Nanostructured Biopolymer Matrix Reinforced with TiO2 and Essential Oil: Application for Preservation of Refrigerated Meat. *Food Chem* **2020**, *322*, 126782.
(76) Domínguez, R.; Pateiro, M.; Gagaoua, M.; Barba, F. J.; Zhang, W.; Lorenzo, J. M. A Comprehensive Review on Lipid Oxidation in Meat and Meat Products. *Antioxidants* **2019**, *8* (10), 1−31.
(77) Reitznerová, A.; Uleková, M.; Nagy, J.; Marcinčák, S.; Semjon, B.; Čertík, M.; Klempová, T. Lipid Peroxidation Process in Meat and Meat Products: A Comparison Study of Malondialdehyde Determination between Modified 2-Thiobarbituric Acid Spectrophotometric Method and Reverse-Phase High-Performance Liquid Chromatography. *Molecules* **2017**, *22* (11), 1988.
(78) Kakaei, S.; Shahbazi, Y. Effect of Chitosan-Gelatin Film Incorporated with Ethanolic Red Grape Seed Extract and Ziziphora Clinopodioides Essential Oil on Survival of Listeria Monocytogenes and Chemical, Microbial and Sensory Properties of Minced Trout Fillet. *LWT - Food Sci. Technol.* **2016**, *72*, 432−438.

https://doi.org/10.1021/acsfoodscitech.5c00238
ACS Food Sci. Technol. 2025, 5, 2430−2443